Non-Linear Modeling of Active or Passive Optical Lamellar Nanostructures

Alexander V. Kildishev,[a] and Xingjie Ni[a,*]
[a] Birck Nanotechnology Center, School of Electrical and Computer Engineering
Purdue University, West Lafayette, IN 47907, USA

ABSTRACT

A universal approach to modeling the refraction of a monochromatic plane wave incident on an optical metamaterial arranged of arbitrary (passive, active, or plasmonic) layers of linear or feebly non-linear elemental materials is examined. The approach is built on an alternative formulation of the method of single expression, which works well upon different combinations (non-linear lossy dielectric, graded-index Kerr medium, and gain medium with metal) upon either p-polarized or s-polarized light. We show that although the formulation for s-polarized light is straightforward, the p-polarization case is more complicated, since solving an implicit material equation is required. Numerical validation of the proposed method indicates good agreement with the results taken from other numerical solvers (based on finite element and mode matching methods).

Keywords: method of single expression, non-linear optics, optical metamaterials

1. INTRODUCTION

The latest progress in the numerical analysis [1], fabrication and optical characterization [2] of low-loss nanostructured optical lamellar media with an effective hyperbolic dispersion has been inspired by the intriguing properties of the perfect focusing device with compensated losses [3]. Most recently, other promising optical effects, made possible through the use of hyperbolic metamaterials (HMMs), has come into focus. It was reported that HMMs can have a unique broadband singularity in the photonic density of states (PDOS) [4]. For example, because spontaneous emission depends appreciably on the available photonic density of states, the emission was predicted to be enhanced close to the surface of HMM. Not only could such materials enhance the spontaneous emission (e.g., of a quantum dot), but could also cause the photons to be emitted in a given direction.

For these reasons, there is considerable interest in accurate, computationally inexpensive, and hence presumably one-dimensional tools for modeling the dynamics of plane waves in a most general HMM structure. The approach should include an adequate treatment of the layers with a weak non-linearity, gain, gradients of the refractive index, losses, and plasmonic effects. A method of single expression (MSE, [5, 6]) has a promise to satisfy all of the above requirements. Here, we are extending this practical concept to be capable of modeling any planar lamellar nano-structures with effective hyperbolic dispersion. The proposed alternative formulation of MSE could be used to design HMMs that are optimized to have specific absorption, reflection and transmission spectra and given non-linear responses to light waves. Subsequently, the development of a nanophotonic modeling tool shall be undertaken, with a goal of substituting or complementing our current software tools for linear cases [7, 8].

A lamellar strucure has been used to validate the approach with numerical simulations of a multilayer stack of silver-dielectric layers with nanoscale thicknesses. Full-wave electromagnetic simulations have been completed using a commercial finite-element software and our SHA technique [7, 9], and the validation results are in good agreement with those obtained from the proposed method.

2. THE METHOD OF SINGLE EXPRESSION

2.1 Nomenclature

Throughout the paper we use the following free-space constants: wavelength $\lambda[\mathrm{m}]$, wavenumber $k = 2\pi/\lambda[\mathrm{rad/m}]$,

* xni@purdue.edu; phone 1 (765) 496 3308; fax 1 (765) 496-2018
Optical Complex Systems: OCS11, edited by Gérard Berginc, Proc. of SPIE Vol. 8172
81720A · © 2011 SPIE · CCC code: 0277-786X/11/$18 · doi: 10.1117/12.898740

the speed of light, $c = 299792458[\mathrm{m/s}]$, permeability $\mu_0 = 4\pi\times10^{-7}[\mathrm{H/m}]$, permittivity $\varepsilon_0 = c^{-2}/\mu_0[\mathrm{F/m}]$, and impedance $z_0 = \mu_0 c[\Omega]$. We shall also note that the normalized 2D space ($kx \to x$, $ky \to y$) and the corresponding derivatives (denoted as superscript indices in parenthesis) are used in the paper. Figure 1 shows a general set-up of the problem for two distinct linear polarizations of light; s-polarized incidence is shown in panel (a), while the p-polarization case is shown in (b).

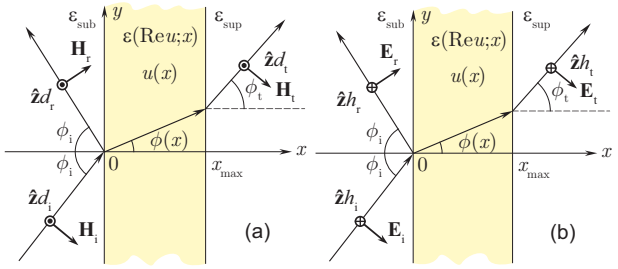

Fig. 1. General set-up of the problem for two distinct linear polarizations of light; (a) *s*-polarized, and (b) *p*-polarized incidence.

2.2 Alternative formulation for s-polarization

We start with the monochromatic scalar wave equation $d^{(x,x)} + d^{(y,y)} + \varepsilon d = 0$, which is written for s-polarized light ($\hat{\mathbf{z}}d = \varepsilon_0 \vec{E}$). Following the MSE we consider a test function written as,

$$d = \exp\left[u(x) + v(x)\, y\right],\ \{u, v\} \in \mathbb{C}, \tag{1}$$

which is a different form of the original MSE formulation [1].

Here, a possible non-linearity of permittivity is introduced through additional dependence on $l = \mathrm{Re}\, u$; hence, the complex permittivity, $\varepsilon(l;x) = \varepsilon_l(x) + \chi(l;x)$, allows for lossy or gain elemental materials with sharp or continuous changes in linear permittivity ε_l and non-linear susceptibility χ.

We shall note that $v = \imath\sqrt{\varepsilon}\sin\phi$ is defined by a position-dependent angle $\phi(x)$ and a position-dependent permittivity $\varepsilon(x)$, but in accord with Snell's law, this part is invariant through the slab, i.e. $\sqrt{\varepsilon_i}\sin\theta_i = \sqrt{\varepsilon}\sin\phi = \sqrt{\varepsilon_s}\sin\theta_s$, we finally arrive at ($k_y = \sqrt{\varepsilon_i}\sin\theta_i$):

$$d = \exp\left[u(x) + \imath k_i y\right], \tag{2}$$

converting the scalar wave equation $d^{(x,x)} + d^{(y,y)} + \varepsilon d = 0$ into a classical Riccati equation

$$u^{(x,x)} + \left(u^{(x)}\right)^2 + \varepsilon(l;x) - k_y^2 = 0. \tag{3}$$

2.3 Alternative formulation for p-polarization

In contrast with s-polarized incidence, for the p-polarization, there is a complication due to an implicit material equation [10, 11]. First, using $h = \exp\left[u(x) + \imath k_y y\right]$, we write

$$\left\{\begin{array}{l} \nabla\cdot\left[\varepsilon^{-1}\nabla h\right] + h = 0 \\ \varepsilon^{(x)} = \varepsilon_l^{(x)} + \left[\chi\left(|\nabla h|, |\varepsilon|\right)\right]^{(x)} \end{array}\right\}, \tag{4}$$

which is equivalent to

$$\left\{\begin{array}{l} u^{(x,x)}+\left(u^{(x)}\right)^2-\left(\ln\varepsilon\right)^{(x)}u^{(x)}+\varepsilon-k_y^2=0 \\ g^{(x)}=\left|\nabla h\right|^{(x)}=\left(e^{\mathrm{Re}u}\sqrt{\left|u^{(x)}\right|^2+k_y^2}\right)^{(x)} \\ \varepsilon^{(x)}=\varepsilon_l^{(x)}+\chi^{(g)}g^{(x)}+\chi^{(|\varepsilon|)}\left|\varepsilon\right|^{(x)} \end{array}\right\}, \tag{5}$$

where the logarithmic derivative is $\left(\ln\varepsilon\right)^{(x)}=\varepsilon^{(x)}/\varepsilon$.

2.4 Cubic non-linearity for p-polarization

As an example, we may consider a cubic non-linearity ($g^2=\left|\nabla h\right|^2=\left(\left|u^{(x)}\right|^2+k_y^2\right)^2e^{2\mathrm{Re}u}$)

$$\varepsilon=\varepsilon_l+3\chi^{(3)}z_0^2g^2\left|\varepsilon\right|^{-2}. \tag{6}$$

Then, the above gives $\left[\left(\varepsilon\bar{\varepsilon}\right)\left(\varepsilon-\varepsilon_l\right)\right]^{(x)}=3\chi^{(3)}z_0^2\left(g^2\right)^{(x)}$, or $\alpha\ln\varepsilon^{(x)}+\ln\bar{\varepsilon}^{(x)}\beta=\gamma$, where $\alpha=\varepsilon+\beta$, $\beta=\varepsilon-\varepsilon_l$, and $\gamma=\varepsilon_l^{(x)}+3\chi^{(3)}z_0^2\left(g^2\right)^{(x)}\left|\varepsilon\right|^{-2}$, and we finally arrive at,

$$\varepsilon^{(x)}=\varepsilon\left(\gamma\bar{\alpha}-\bar{\gamma}\beta\right)\Big/\left(\left|\alpha\right|^2-\left|\bar{\beta}\right|^2\right). \tag{7}$$

Hence, the general scheme degenerates into the following sequence,

$$\left\{\begin{array}{l} u^{(x,x)}+\left(u^{(x)}\right)^2-\left(\ln\varepsilon\right)^{(x)}u^{(x)}+\varepsilon-k_y^2=0 \\ \left(g^2\right)^{(x)}=e^{2\mathrm{Re}u}\left(u^{(x)}\bar{u}^{(x,x)}+\bar{u}^{(x)}u^{(x,x)}+2\,\mathrm{Re}\,u^{(x)}\left[\left|u^{(x)}\right|^2+k_y^2\right]\right) \\ \ln\varepsilon^{(x)}=\left(\gamma\bar{\alpha}-\bar{\gamma}\beta\right)\Big/\left(\left|\bar{\alpha}\right|^2-\left|\beta\right|^2\right) \end{array}\right\} \tag{8}$$

Only if the change of ε is adiabatic, i.e. $\left(\ln\varepsilon\right)^{(x)}\to 0$, then (8) can be reduced to (3).

2.5 Initial conditions for linear polarized light

At the substrate side of the slab at $y=0$, we take either $d=d_{\mathrm{t}}=d_{\mathrm{t},0}\exp\left(-\imath k_{\mathrm{sub}}x_{\max}\right)$ for s-polarization, or $h=h_{\mathrm{t}}=h_{\mathrm{t},0}\exp\left(-\imath k_{\mathrm{sub}}x_{\max}\right)$ for p-polarization, and the general initial condition for u is $u\left(x_{\max}\right)=-\imath k_{\mathrm{sub}}x_{\max}$, where $k_{\mathrm{sub}}=\sqrt{\varepsilon_{\mathrm{sub}}-k_y^2}$.

At the illumination side, we may use the Sommerfeld radiation condition,

$$\begin{array}{l} d_{\mathrm{i}}=\frac{1}{2}\left(d-\imath n_{\mathrm{sup}}^{-1}d^{(x)}\right) \\ d_{\mathrm{r}}=\frac{1}{2}\left(d+\imath n_{\mathrm{sup}}^{-1}d^{(x)}\right) \end{array}, \tag{9}$$

thus splitting the incident and the reflected fields (d_{i}, d_{r}), and obtaining their magnitudes. Finally, using (2) in (9) for $y=0$, we arrive at:

$$\begin{array}{l} d_{\mathrm{i}}=\frac{1}{2}\left(1-\imath n_{\mathrm{sup}}^{-1}u^{(x)}\right)\exp u \\ d_{\mathrm{r}}=\frac{1}{2}\left(1+\imath n_{\mathrm{sup}}^{-1}u^{(x)}\right)\exp u \end{array}. \tag{10}$$

3. VALIDATION TEST

The proposed method is implemented using the explicit Runge-Kutta scheme. A metal-dielectric multilayer structure arranged of alternating layers of silver and Vanadium Pentoxide (V_2O_5) as shown in Fig. 2 is designed for the validation test. The thickness of each silver layer is 20 nm. The thickness of the external V_2O_5 layers is 28 nm, while the thickness of other V2O5 layers is 64 nm; the entire structure is immersed in air. The plane wave of the incident light propagates normally to the interface from left to right. V_2O_5 exhibits strong cubic nonlinearity with the value of $\chi^{(3)}$ about 31×10^{-8} e.s.u. and a linear refractive index of 2.37 at a wavelength of 532 nm [12]. The optical constants of silver are taken from [13].

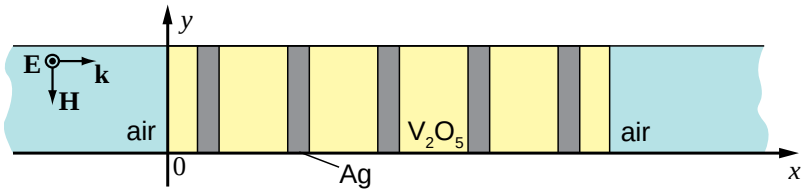

Fig. 2. Metal-dielectric multilayer structure arranged of alternating layers of silver and Vanadium Pentoxide (V_2O_5) for the validation test. The thickness of each silver layer is 20 nm. The thickness of the external V_2O_5 layers is 28 nm, while the thickness of other V2O5 layers is 64 nm. The entire structure is immersed in air.

The linear case, where V_2O_5 layers were treated as dielectric layers without any nonlinearity, has been tested first. The resulting transmittance and reflectance spectra are shown in Fig. 3(a). Full-wave electromagnetic simulations have been also carried out using our SHA approach [9], and the validation results are in good agreement with those obtained from the proposed method. Simulations considering cubic nonlinearity have been carried out at a wavelength of 532 nm. Fig. 3(b) shows transmittance and reflectance vs. the E-field magnitude. The result obtained from a commercial finite element method (FEM) software package (COMSOL Multiphysics) is also included in Fig. 3(b) as a reference. Note that as shown in the figure the nonlinear solver in FEM fails to obtain a valid solution for the input electric field magnitude larger than 2.45×10^7 V/m. From the figure we can clearly see there is strong nonlinear effect due to the change of the strength of the input field. The results obtained from the proposed method and those obtained from FEM solver match quite well with each other.

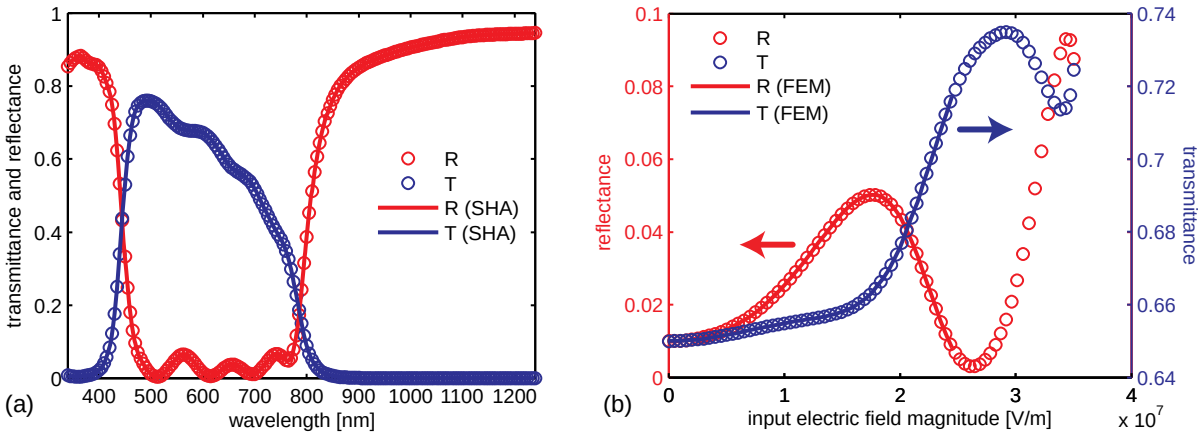

Fig. 3. Comparison of (a) transmittance and reflectance spectra, and (b) input field strength dependent transmittance and reflectance obtained by using the proposed method and other methods.

Furthermore, the transmittance and reflectance spectra with different angle of incidence are calculated using the proposed method and SHA approach. The results which are shown in Fig. 4(a) indicate a very good agreement between the two methods. We also show the input electric field dependent spectra with different angle of incidence in Fig. 4(b).

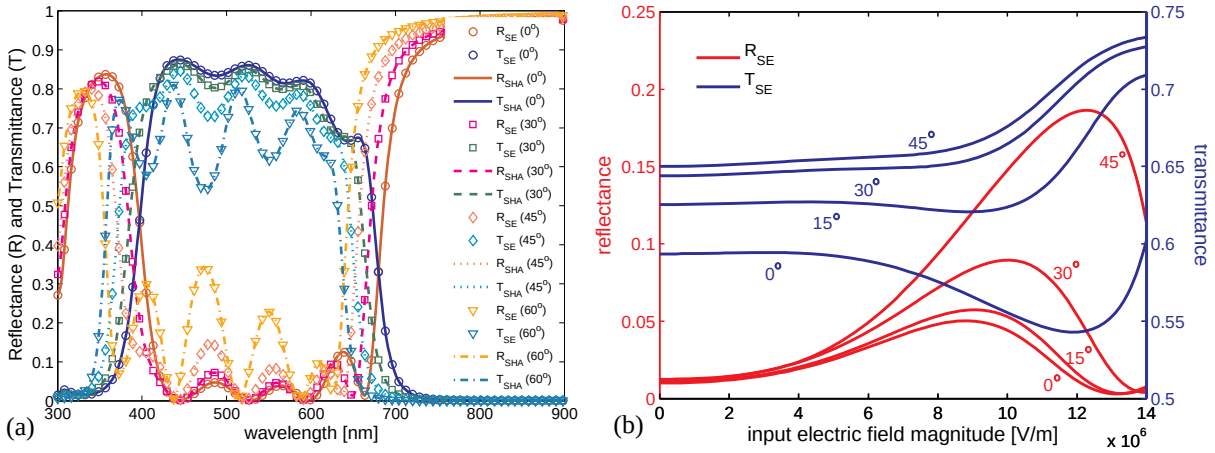

Fig. 4. (a) Comparison of transmittance and reflectance spectra with different incidence angle at a wavelength of 532 nm. (b) Input electric field magnitude dependent transmittance and reflectance with different incidence angle at a wavelength of 532 nm.

Most interestingly, the structure we studied above shows a bistability behavior for sufficiently large input electric field magnitude. Fig. 5 shows this behavior and the arrows show the abrupt changing of the reflectance or transmittance when the magnitude of the input electric field increases or decreases. The phenomenon has been studied in nonlinear materials for a long time and similar behavior was discussed for multilayer structures [6, 14]. With our proposed method, we are able to capture this bistability behavior precisely.

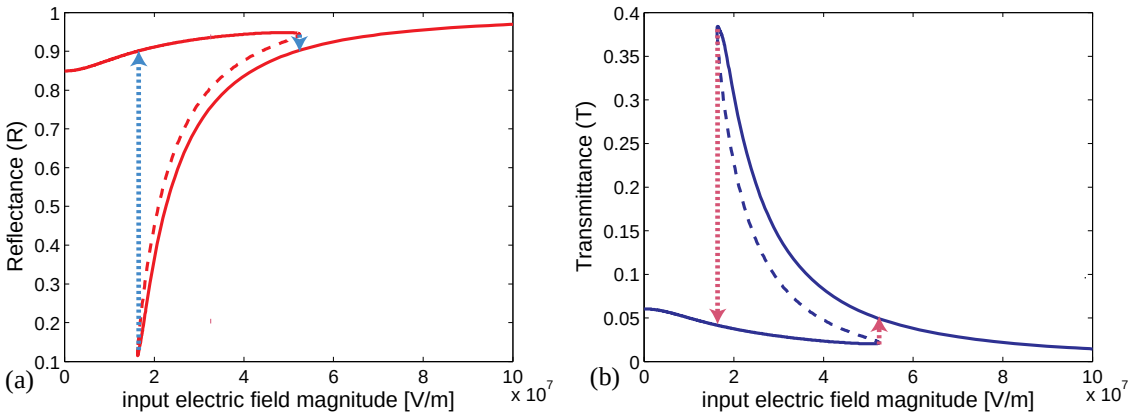

Fig. 5. Input electric field strength dependent (a) reflectance and (b) transmittance shows bistability, the branching happens when the input electric field reaches a sufficiently high value. The dotted lines with arrows show the abrupt changing of the reflectance or transmittance when the magnitude of the input electric field increases or decreases.

Another example we want to show in this paper is an active metal-dielectric multilayer HMM which consists of 16 layers of alternating 6-nm-thick silver layers and 50-nm-thick active dielectric layers on a glass substrate. The size-dependent sliver loss has been taken into account by setting the loss factor to two [15]. For the active dielectric medium, we take the experimentally measured gain values of the organic dye (Rh800) mixed in epoxy [16]. The refractive index of epoxy is 1.65. The emission peak of Rh800 is about 720 nm. The gain coefficient of a material is proportional to the imaginary part of the refractive index, we therefore modeled the active dielectric with a complex dielectric function. The effective anisotropic permittivities are shown in Fig. 6. At a wavelength around 730 nm, we can clearly see that the multilayer structure shows a hyperbolic dispersion, namely the effective permittivities are having different signs in x and y directions. The “without gain” case is studied by simply taking pure epoxy as the material of the dielectric layers.

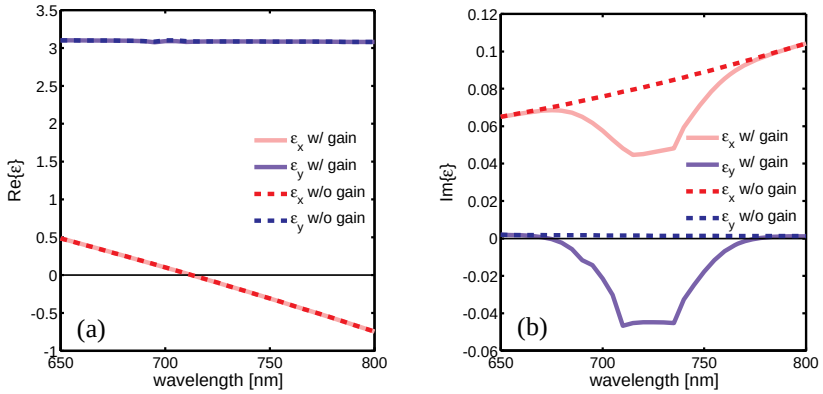

Fig. 6. Effective anisotropic permittivity calculated from SHA for a silver-dielectric HMM with gain (solid line) and without gain (dashed line). (a) real part of permittivity and (b) imaginary part of permittivity.

Fig. 7(a) shows the transmittance and reflectance spectra for this metal-dielectric multilayer HMM with and without gain using proposed method and SHA. The spectra shows that the absorptance for the HMM with gain is a little bit lower than that of without gain at around 720 nm which is the active wavelength range. Fig. 7(b) shows the transmittance, reflectance, and absorptance versus incident angle at a wavelength of 730 nm for the HMM. We can see that the effect of the gain reduces with increasing incident angle. In all the cases, the results from the proposed method show perfect agreement with those from SHA.

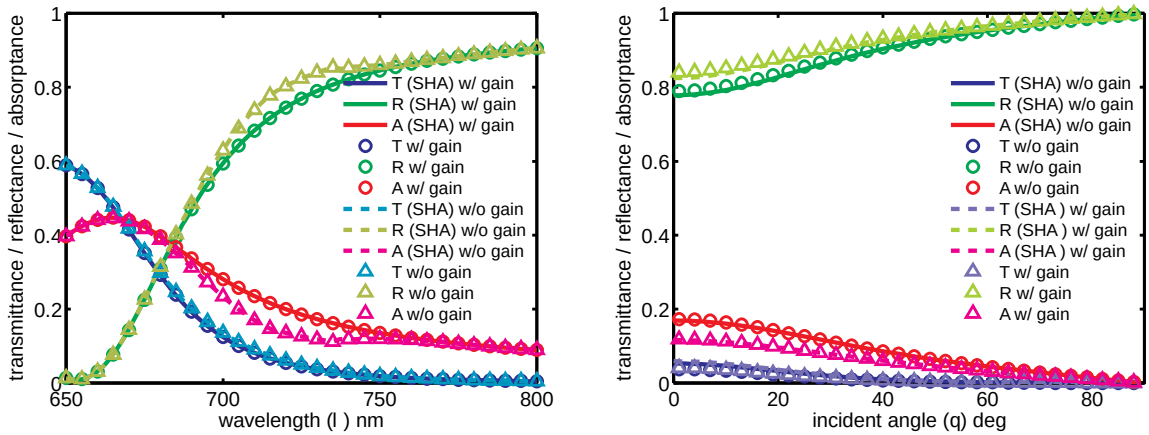

Fig. 7. Comparison of (a) transmittance and reflectance spectra, and (b) angular dependent transmittance and reflectance at a wavelength of 730 nm, obtained by using the proposed method and SHA with/without gain for metal-dielectric multilayer HMM.

4. SUMMARY

A general approach to modeling the propagation of a plane wave through an arbitrary lamellar nanostructure has been obtained using a modified method of single expression. The new formulation presents either the electric or magnetic scalar wave as $\exp\left[u(x)+\imath k_{\mathrm{i}} y\right]$, thus transforming the wave equation into the general dispersion identities (Eqs. (3) and (4)) for s-polarized and p-polarized light respectively. For the trivial case of homogeneous media both equations reduce to the standard dispersion relation, $\imath u^{(x)} = k_x = \sqrt{\varepsilon - k_y^2}$. We note that in contrast to the s-polarization case, which is quite straightforward, the p-polarization case is complicated with an implicit material equation, which can be converted into an explicit form within a selected numerical scheme.

By controlling the parameters of the numerical scheme, (e.g., by reducing the minimal step-size) the convergence of the simulation approach has been additionally analyzed. This study has also shown that it is possible to apply the MSE to very different combinations of the elemental materials in a given lamellar structure, thus allowing for an arbitrary

mixture of layers (metals, dielectrics with gain, dielectrics with non-linear optical properties of other origin) with gradient-index structures, and giving a tool for designing hyperbolic metamaterials for near field optical imaging and other applications.

5. ACKNOWLEDGEMENT

This work was supported by ARO MURI Awards 50342-PH-MUR.

REFERENCES

[1] M. P. H. Andresen, A. V. Skaldebo, M. W. Haakestad *et al.*, "Effect of gain saturation in a gain compensated perfect lens," Journal of the Optical Society of America B-Optical Physics 27(8), 1610-1616 (2010).

[2] W. Q. Chen, M. D. Thoreson, S. Ishii *et al.*, "Ultra-thin ultra-smooth and low-loss silver films on a germanium wetting layer," Optics Express 18(5), 5124-5134 (2010).

[3] S. A. Ramakrishna, and J. B. Pendry, "Removal of absorption and increase in resolution in a near-field lens via optical gain," Physical Review B 67(20), 201101 (2003).

[4] I. I. Smolyaninov, and E. E. Narimanov, "Metric Signature Transitions in Optical Metamaterials," Physical Review Letters 105(6), 067402 (2010).

[5] H. V. Baghdasaryan, and T. M. Knyazyan, "Problem of plane EM wave self-action in multilayer structure: an exact solution," Optical and Quantum Electronics 31(9-10), 1059-1072 (1999).

[6] H. V. Baghdasaryan, and T. M. Knyazyan, "Modelling of strongly nonlinear sinusoidal Bragg gratings by the Method of Single Expression," Optical and Quantum Electronics 32(6-8), 869-883 (2000).

[7] X. Ni, Z. Liu, F. Gu *et al.*, "PhotonicsSHA-2D: Modeling of Single-Period Multilayer Optical Gratings and Metamaterials," doi:10254/nanohub-r6977.6 (2009).

[8] S. Ishii, U. K. Chettiar, X. Ni *et al.*, "PhotonicsRT: Wave Propagation in Multilayer Structures," doi:10254/nanohub-r5968.14 (2008).

[9] X. Ni, Z. Liu, A. Boltasseva *et al.*, "The validation of the parallel three-dimensional solver for analysis of optical plasmonic bi-periodic multilayer nanostructures," Applied Physics A: Materials Science & Processing 100(2), 365-374 (2010).

[10] A. V. Kildishev, and N. M. Litchinitser, "Efficient simulation of non-linear effects in 2D optical nanostructures to TM waves," Optics Communications 283(8), 1628-1632 (2010).

[11] K. Alexander V, "Modeling nonlinear effects in 2D optical metamagnetics," Metamaterials 4(2-3), 77-82.

[12] M. Ando, K. Kadono, M. Haruta *et al.*, "Large 3rd-Order Optical Nonlinearities in Transition-Metal Oxides," Nature 374(6523), 625-627 (1995).

[13] X. Ni, Z. Liu, and A. V. Kildishev, "PhotonicsDB: Optical Constants," doi:10254/nanohub-r3692.6 (2008).

[14] C. J. Herbert, and M. S. Malcuit, "Optical Bistability in Nonlinear Periodic Structures," Optics Letters 18(21), 1783-1785 (1993).

[15] Z. Liu, K.-P. Chen, X. Ni *et al.*, "Experimental verification of two-dimensional spatial harmonic analysis at oblique light incidence," J. Opt. Soc. Am. B 27(12), 2465-2470 (2010).

[16] S. Xiao, V. P. Drachev, A. V. Kildishev *et al.*, "Loss-free and active optical negative-index metamaterials," Nature 466(7307), 735-738 (2010).